ORIGINAL CONTRIBUTION

One-dimensional array of nanoparticles using segmented polyurethane nanofibers as a template for enhanced catalytic efficiency

Taichi Meboso[1] · Satoshi Goto[2] · Eiichiro Takamura[2] · Hiroaki Sakamoto[2]

© The Author(s) 2023

Abstract

Metal nanoparticles are used to catalyze chemical reactions. Among them, noble metal nanoparticle catalysts need to be used in small quantities. Some reports reveal catalytic activity is further improved by controlling nanoparticle arrangement and distribution. Much research has been directed toward the formation of one-dimensional arrays by compositing metal nanoparticles with template materials. However, previously reported methods form arrays that lack linearity or suitable interparticle distances, which is ascribable to array crossover and particle aggregation, in addition their fabrication procedures are expensive and not suitable for large-scale practical use. Here we show that one-dimensional arrays of platinum nanoparticles (PtNPs) were formed by using electrospun polyurethane nanofibers as a template. PtNPs adsorbed on each polyurethane nanofiber form a one-dimensional array over longer distances. The catalytic H_2O_2 decomposition performance of the prepared one-dimensional PtNP arrays was 45.6% decomposition in 15 min, which revealed a decomposition rate more than twice that obtained using the same number of PtNPs randomly distributed on the template or dispersed in a liquid. Although this method is a very simple method for one-dimensional arrangement of metal nanoparticles, thereby improving catalytic efficiency per metal nanoparticle, which help to reduce the amount of metal nanoparticles used during catalysis and contributes the cost of catalysis products cost.

Keywords Nanoparticle · One-dimensional array · Polyurethane nanofiber · Platinum · Catalysis

Introduction

Nanotechnology is gaining increasing attention, nanoparticles becoming more-actively researched [1–7]. Catalysis, especially involving metal nanoparticles, has been among the most actively investigated nanoparticle fields [8–15]. Such a catalyst reduces the activation energy of a reaction but is not included in the product; consequently, a small amount of a catalyst is preferred from the perspectives of reducing cost and minimizing impurities. The beginning of nanoparticulation of bulk metals is to increase the specific surface area and improve the catalytic efficiency [16]. In addition, recent reports reveal that catalytic efficiency is related to metal nanoparticle distribution [17–20]. Thus, the catalyst becomes more efficient when the particles are widely spaced rather than aggregated. Therefore, controlling the inter-particle distance is one of the key parameters for enhancing the catalytic activity. And more, noble metal nanoparticulation and distribution control can significantly affect cost when a noble metal is used as the catalyst.

Controlling the metal nanoparticle distribution on the templates is a core nanomaterials chemistry problem, and many one-dimensional array templates have been used to assemble ordered nanoparticle aggregate, with DNA, self-assembled polymers, carbon nanotubes, and lithography used to form templates [21–29]. However, DNA and lithography involve expensive procedures that are not suitable for large-scale practical use. Self-assembled polymers and carbon nanotubes procedure that lack linearity or suitable interparticle distances due to array crossover and nanoparticle aggregation.

✉ Hiroaki Sakamoto
hi-saka@u-fukui.ac.jp

[1] Advanced Interdisciplinary Science and Technology, Graduate School of Engineering, University of Fukui, 3-9-1Fukui Prefecture, Bunkyo, Fukui City 910-8507, Japan

[2] Frontier Fiber Technology and Science, Graduate School of Engineering, University of Fukui, 3-9-1Fukui Prefecture, Bunkyo, Fukui City 910-8507, Japan

To overcome these problems, our group introduced one-dimensional arrays of nanoparticles fabricated using electrospun segmented polyurethane (PU) nanofibers as a template [30]. A surface specific segmented PU nanofiber structure was achieved by stretching (stretched PU nanofibers) during electrospinning [31]. In these reports, hard segments are linearly distributed along the long axis of the fiber by the hard and soft segments of the PU molecular structure to form a remarkable phase-separated structure. This is ascribable to the stretching force applied during the electrospinning preparation of the PU nanofiber. Furthermore, these reports revealed that gold nanoparticles can be one-dimensionally arranged on hard segments that are linearly distributed along the long axis of the fiber through hydrophobic interactions. Compared to previous methods, this method enables uniform interparticle distances and linearity to be maintained over long distances. Moreover, the most significant feature of this method is simplicity: a one-dimensional array of nanoparticles is assembled using inexpensive PU as a template, with the PU nanofibers simply dipped into a nanoparticle dispersion.

In the present study, we assembled one-dimensional arrays of platinum nanoparticles (PtNPs) using stretched PU nanofibers as a template. In addition, we demonstrated that the PtNP-controlled distribution facilitated by this method significantly improves catalytic efficiency compared to that of the non-controlled (randomly dispersed) distribution. Some recent reports have shown that catalytic efficiency is related to metal nanoparticle distribution, with interparticle distance or nanoparticle (or atom/molecule) arrangement used to control the electronic state of the particle surface or adsorption of the substrate. We assume that one-dimensional PtNP arrays can similarly affect catalytic efficiency by arranging PtNPs using our method.

Experimental

Chemicals and materials

PU pellets (Elastollan 1180A; 77,000, Mw/Mn = 1.89) were purchased from BASF Japan (Tokyo, Japan), glass substrates ($20 \times 20 \times 1$ mm) from AS ONE (Osaka, Japan), Cu grid mesh from Okenshoji (Tokyo, Japan), tetrahydrofuran (THF), *N,N*-dimethylformamide (DMF), Sulfuric acid (H_2SO_4) and hydrogen peroxide (H_2O_2) from FUJIFILM Wako Chemicals (Osaka, Japan). Carbon nanotube multi-walled (MWCNT; $\varphi = 20-40$ nm, L = $1-2$ μm) was purchased from Tokyo Chemical Industry. PtNPs ($\varphi = 2$ nm) were purchased from TANAKA Precious Metals (Tokyo, Japan) as 4wt% aqueous nitric acid dispersion. The surfaces of the PtNPs were coated with polyvinylpyrrolidone (PVP), with ethyl terminal groups. The PtNPs surface coated with

PVP, which has a methyl group at the terminal, was chosen to adsorb via hydrophobic interactions on the hydrophobic portion of the electrospun PU nanofibers [30]. H_2O_2 assay kit was used Amplite Colorimetric Hydrogen Peroxide Assay Kit (ABD AAT Bioquest, US). Electrospinning devices were from MECC (Fukuoka, Japan), High voltage unit; HVU-30P100, Collector; C-DI, Spinneret; S-TU/100/5 mL.

Preparation of PU nanofibers

An 8% (w/v) solution of PU in a 95:5 (v/v) mixture of THF and DMF was prepared by stirring overnight at room temperature. It was visually confirmed that all pellets were dissolved and there was no phase separation of the solution. PU nanofibers were fabricated by electrospinning. A high voltage (25 kV) was applied between the syringe needle (27 G) and the ground electrode. A rotating collector ($\varphi = 100$ mm) was placed horizontally 100 mm from the needle, and the PU solution was extruded from the syringe at 1.0 mL h^{-1}. The rotational speed and spinning duration were 2000 rpm and 4 h, respectively, for stretched nanofibers, and 0 rpm (stationary) and 2 h, respectively, for unstretched nanofibers. To prepare MWCNT-containing PU nanofibers, the MWCNTs were dispersed in a PU solution and subjected to 28 kHz ultrasonic treatment for 2 h before spinning. The spinning duration was 30 min for both, the unstretched and stretched nanofibers.

All synthesized samples were dried and stored in a desiccator. The PU nanofibers were electrospun onto glass substrates for scanning electron microscopy (SEM) and catalytic efficiency investigation, and Cu grid mesh for transmission electron microscopy (TEM).

Platinum nanoparticles adsorption on PU nanofiber surface

The purchased PtNPs were diluted with Milli-Q water to 14.8×10^{-3} wt%. The fiber-spun substrates were placed in the dilute PtNP dispersion with the fiber surfaces downward for 12 h. The substrates were then washed with Milli-Q water and dried overnight in a desiccator.

Scanning electron microscopy

The fabricated PU nanofibers were coated with Au/Pd using an ion coater (VACCUM DEVICE, Japan, MSP-1S) and subject to SEM with an accelerate voltage 15 kV (JEOL, Japan, JSM-6390). The diameters of the nanofibers were determined from the SEM images (5–10 k magnification) using ImageJ software.

Transmission electron microscopy

The PtNP-adsorbed PU nanofibers were subjected to TEM (Hitachi, Japan, H-7650) at an accelerator voltage of 80 kV. Interparticle distances were determined from TEM images (50 k magnification) using ImageJ software.

Determining the amount of adsorbed PtNPs

The number of PtNPs adsorbed per unit nanofiber was determined using laser ablation inductively coupled plasma mass spectrometry (LA-ICP-MS: LA part; ST. JAPAN INC., Japan, Jupiter Solid Nebulizer, ICP-MS part; Thermo Fisher, Japan, iGAP-TQ). Samples were ablated in raster mode with a sample-surface fluence of 5 J cm^{-2}, a repetition rate of 1 Hz, and a laser spot size of 1×1 mm. Helium gas was used as the carrier gas, and argon gas was used to ablate the sample. A 30 s ICP-MS time was used and laser ablation was performed 5 s after the start of the ICP-MS experiment. The Pt/C intensity ratio and the number of Pt nanoparticles were calculated by analyzing the LA-ICP-MS signal intensity; the former was determined from corresponding peak areas, while the number of adsorbed PtNPs per unit C was determined from a calibration curve constructed using samples of known concentration (v/v%), Pt density, and PtNP volume. The calculated data are reported as means $\pm$ standard deviations.

Catalytic efficiency

PtNP catalytic efficiency was evaluated based on the ability to decompose H_2O_2. The purchased 30% H_2O_2 solution was diluted to 50 µM with Milli-Q water, after which 3 mL this solution was added to a petri dish, and the PtNP-adsorbed PU nanofibers were immersed in the solution at room temperature for 15 min. The H_2O_2 solution was sampled, and the concentration of H_2O_2 was determined using a colorimetric assay kit. The assay kit solution included Amplite™ IR peroxidase substrate, horseradish peroxidase, and dimethyl sulfoxide (DMSO). The 50 µL assay kit solution was added in 96-well plate. Add 50 µL H_2O_2 sample solution to each well. The test samples to make the total H_2O_2 assay volume of 100 µL/well. Incubation the reaction at room temperature for 10 min, protected from light. Monitor the absorbance with a microplate reader (Thermo Fisher Scientific K. K., Japan, Multiskan Sky High) at 650 nm.

The electrochemical catalytic surface area (ECSA) was estimated through cyclic voltammetry (CV). CV was performed using an electrochemical analyzer (BAS, Japan, ALS660E) and a three-electrode method with PtNP-adsorbed PU nanofibers (unstretched or stretched) as the working electrode, Ag/AgCl (BAS, Japan, RE-1B) as the reference electrode, and a Pt wire (Nilaco, Japan, PT-351384) as the counter electrode. The measurement conditions involved the use of a 0.5 M H_2SO_4 electrolyte, -0.25 V−1.2 V sweep range, and 0.1 V/s sweep rate. Before the measurement, a degassing operation was carried out by bubbling N_2 gas through the solution for 30 min.

Results and discussion

Characterization of the PtNP-adsorbed PU nanofibers

Figure 1a and b shows the SEM images of PtNP-adsorbed PU nanofibers and Fig. 1c shows the histograms of nanofibers diameter determined by SEM images. The average

Fig. 1 **a**, **b** SEM images of PtNP-adsorbed PU nanofibers. **a** unstretched, **b** stretched. **c** Histograms of nanofibers diameter. Horizontal axis is particle diameter, vertical axis is number of particles
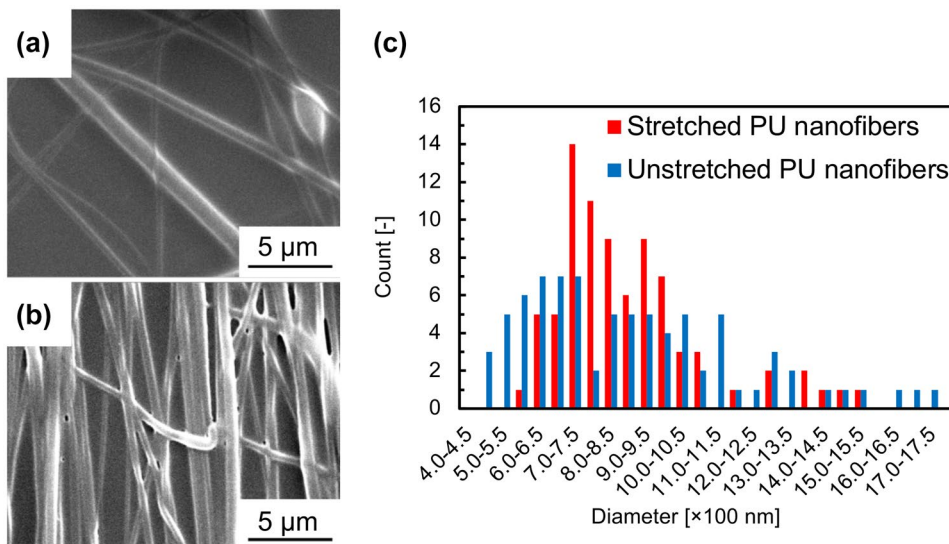
Fig. 2 TEM images of PtNPs on single **a** unstretched and **b** stretched PU nanofibers. The red circle surrounds the agglomeration of particles
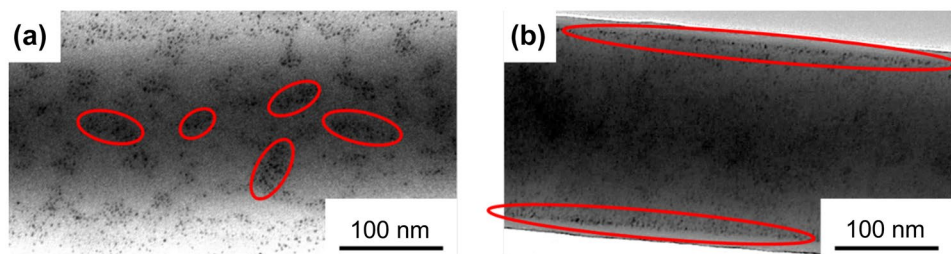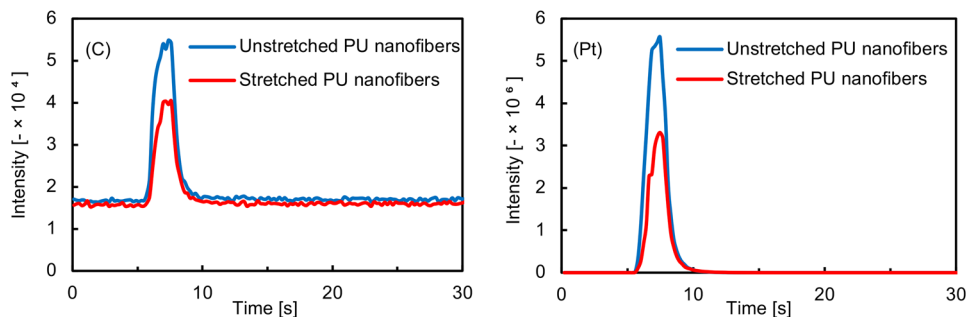

Fig. 3 LA-ICP-MS trace of carbon (C) and platinum (Pt) elements

diameter of unstretched nanofibers and stretched nanofibers are 880.8 ± 298.0 nm and 871.8 ± 203.3 nm, respectively. Figure 2 shows TEM images of PtNP-adsorbed PU nanofibers. At the unstretched PU nanofibers, PtNPs were adsorbed on hard segments as clusters of several PtNPs that were randomly distributed on the surfaces of the unstretched PU nanofibers (Fig. 2a). On the other hand, as the stretched PU nanofibers, PtNPs were adsorbed on hard segments in a one-dimensional manner along the long axis of stretched PU nanofiber (Fig. 2b). Furthermore, PtNPs adsorbed on the stretched PU nanofibers were observed to be continuously adsorbed along both edges of the fiber in the TEM image. PtNPs with interparticle distances of less than 10 nm are shown enclosed in red boundaries, and their aspect rations were measured to compare the linearities and lengths of the arrays in the two TEM images. Aggregated PtNPs with low aspect ratios aggregate into ellipse like structures, while those with high aspect ratios form long linear arrangements. The PtNP aggregates adsorbed on the unstretched PU nanofibers were an average aspect ratio of 2.6, while that for the PtNPs adsorbed on the stretched PU nanofibers were determined to be 13.4.

Table 1 Pt/C intensity ratios numbers of PtNps adsorbed per unit C

	Unstretched (0 rpm)	Stretched (2000 rpm)
Intensity ratio (Pt/C) [-]	137.6 ± 10.2	35.4 ± 12.6
PtNP adsorption amount [mg/g]	0.897 ± 0.067	0.883 ± 0.082

Numbers of adsorbed PtNPs

The number of adsorbed PtNPs per unit PU nanofiber needs to be evaluated in order to determine whether catalytic efficiency depends on PtNP loading or distribution. Elemental C per unit volume was determined by LA-ICP-MS, with the obtained C signal assumed to belong to carbon chains that form the PU structure. The intensities of the Pt signals were normalized against the C signals of the unstretched and stretched samples LA-ICP-MS traces are displayed in Fig. 3. Table 1 lists the Pt/C intensity ratios and calculated numbers of PtNPs adsorbed per unit C from the data shown in Fig. 3. The Pt/C intensity ratios of the unstretched and stretched nanofibers were determined to be 137.6 ± 10.2 and 135.4 ± 12.6, respectively.
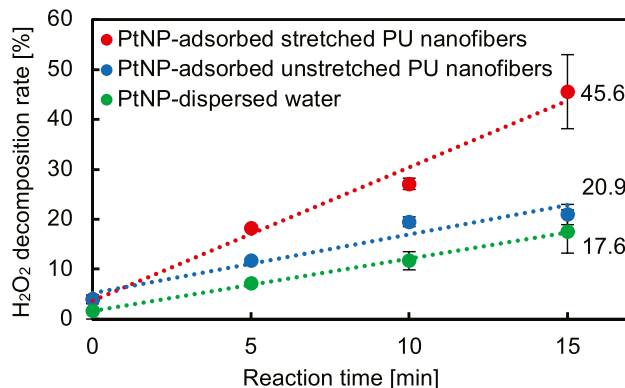

Fig. 4 H_2O_2 decomposition as function of time
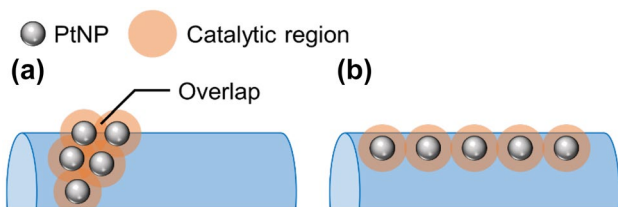
Fig. 5 Depicting overlaps in catalytic regions resulting from controlled distributions of PtNPs. **a** Randomly distributed PtNPs on an unstretched PU nanofiber, **b** One-dimensional arrays of PtNPs on a stretched PU nanofiber

The adsorbed amounts of PtNPs were calculated to be 0.897 ± 0.067 and 0.883 ± 0.082 mg/g for the unstretched and stretched nanofibers, respectively. The Pt/C intensity ratios and PtNP adsorption amount were almost the same for the unstretched and stretched PU nanofibers.

Catalytic efficiency

H_2O_2 decomposition efficiencies were compared with three samples: using PtNPs with controlled one-dimensional distributions adsorbed on stretched PU nanofibers, PtNPs randomly distributed by adsorption on unstretched PU nanofibers, and PtNPs dispersed in water at the same concentration as those adsorbed on the stretched PU nanofibers, as calculated by LA-ICP-MS, the results of which are shown in Fig. 4. When H_2O_2 was exposed to PtNP-dispersed water, it decomposed over time, with 17.6% decomposition observed after 15 min. The PtNP-adsorbed unstretched PU nanofibers decomposed H_2O_2 faster than the PtNP-dispersed water, with a decomposition of 20.9% recorded after 15 min. However, the best results were obtained using the PtNP-adsorbed stretched PU nanofibers, where 45.6% of H_2O_2 decomposed after 15 min, which is more than twice that observed for the PtNP-adsorbed unstretched PU nanofibers. Despite the stretched PU nanofibers having a similar number of adsorbed PtNPs as the

corresponding unstretched nanofibers (as discussed in Section "Numbers of adsorbed PtNPs"), they showed a significant increase in their ability to decompose H_2O_2. Based on the PtNP adsorption amount from Table 1 and the decomposed percentages of H_2O_2 from Fig. 4, the H_2O_2 decomposition per mg of Pt after 15 min was 19.6% for PtNP-dispersed water, 23.3% for the PtNP-adsorbed unstretched PU nanofibers, and 51.6% for the PtNP-adsorbed stretched PU nanofibers. Thus, the date show that the H_2O_2 decomposition rate is affected by the PtNP distribution. Because PtNP-dispersed water is a heterogeneous catalyst, its decomposition efficiency is lower than that of template-immobilized catalysts. The potential PtNP catalytic regions overlap for the PtNPs adsorbed on the unstretched nanofibers because they form aggregates of multiple nanoparticles; hence, its large specific surface area, which is a PtNP feature, cannot be used effectively (Fig. 5a). On the other hand, the catalytic potential regions overlap much less for the PtNPs adsorbed on the stretched PU nanofibers because they are distributed at uniform intervals (Fig. 5b); consequently, more H_2O_2 substrate can be concurrently catalytically decomposed.

To obtain further information regarding the catalytic potential regions, the ECSA was determined. For the investigate of electrochemical properties and conductivity, CV was conducted on glassy carbon electrodes coated with PtNP-adsorbed nanofibers containing MWCNTs, in their unstretched and stretched states. Figure 6 shows the cyclic voltammograms, with the reduction peaks below 0.2 V representing the H_2 adsorption peaks on the Pt surface. The ECSA of Pt can be calculated from the H_2 adsorption peak and Eq. 1 as follows:

$$\text{ECSA}\left[\text{cm}^2{}_{Pt}\right] = Q_H[\mu C]/C_{Had}\left[\mu C/\text{cm}^2{}_{Pt}\right] \qquad (1)$$

where Q_H is the electric charge of H_2 adsorption (μC) and C_{Had} is the H_2 adsorption/desorption electric charge per unit Pt surface area (μC/cm²$_{Pt}$), with C_{Had} generally assumed to be 210 μC/cm²$_{Pt}$. The calculated ECSA were 0.01162 for
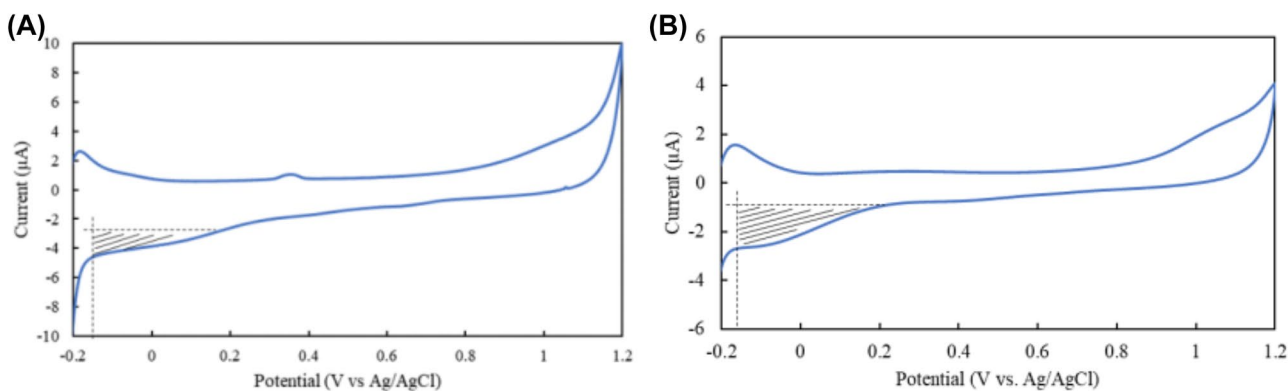

Fig. 6 Cyclic voltammograms of **a** PtNP-adsorbed stretched PU nanofibers and **b** PtNP-adsorbed unstretched PU nanofibers

PtNP-adsorbed unstretched PU nanofibers and 0.0192 cm$^2_{Pt}$ for PtNP-adsorbed stretched PU nanofibers, which shows that the ECSA of stretched one is approximately 1.19 times larger than that of unstretched one. The one-dimensional arrangement of the PtNPs is responsible for the larger catalytically active region, which contributed to the improvement in the H_2O_2 decomposition efficiency.

Conclusions

We assembled one-dimensional arrays of PtNPs using electrospun PU nanofibers as a template. Compared to previous methods, present method maintains uniform interparticle distance and linearity over long distances, which is a significant feature. Moreover, the most important feature of the current method is its simplicity; the one-dimensional arrays of nanoparticles are assembled by dipping an inexpensive PU nanofiber template in to a PtNP dispersion. The assembled one-dimensional arrays of nanoparticles on stretched PU nanofibers decompose H_2O_2 in a significantly more efficient manner than the PtNPs randomly adsorbed on unstretched PU nanofibers and those dispersed in water, despite fewer PtNPs on the stretched PU nanofibers. The PtNP-distributed one-dimensional array decomposed more than twice the amount of H_2O_2 over 15 min than the alternative randomly distributed PtNPs. We hypothesize that the PtNP catalytic regions overlap little in the one-dimensional arrays due to their uniform interparticle distances, which controls distribution in a manner that enables a larger amount of H_2O_2 (as the substrate) to be concurrently catalytically decomposed.

Data availability The datasets generated and/or analyzed during the current study are available from the corresponding author on reasonable request.

Declarations

Conflict of interest The authors declare that they have no conflicts of interest.

References

1. Jeffrey NA, Paige W, H, Olga L, Nilam CS, Jing Z, Richard PVD, (2008) Biosensing with plasmonic nanosensor. Nat Mater 7:442–453. https://doi.org/10.1038/nmat2162
2. Andrew NS, Eugenii K, Itamar W (2000) Nanoparticle Arrays on Surfaces for Electronic, Optical, and Sensor Applications. Chem Phys Chem 1:18–52. https://doi.org/10.1002/1439-7641(20000804)1:1%3c18::AID-CPHC18%3e3.0.CO;2-L
3. Ha NK, Wen XR, Jong SK, Juyoung Y (2012) Fluorescent and colorimetric sensors for detection of lead, cadmium, and mercury ions. Chem Soc Rev 41:3210–3244. https://doi.org/10.1039/c1cs15245a
4. Kyeong SL, Mostafa AES (2006) Gold and Silver Nanoparticles in Sensing and Imaging: Sensitivity of Plasmon Response to Size, Shape, and Metal Composition. J Phys Chem B 110:19220–19225. https://doi.org/10.1021/jp062536y
5. Adam DM, Richard PVD (2003) Single Silver Nanoparticles as Real-Time Optical Sensors with Zeptomole Sensitivity. Nano Lett 3:1057–1062. https://doi.org/10.1021/nl034372s
6. Xiliang L, Aoife M, Anthony JK, Malcolm RS (2006) Application of Nanoparticles in Electrochemical Sensors and Biosensors. Electroanalysis 18:319–326. https://doi.org/10.1002/elan.200503415
7. Juewen L, Yi L (2006) Preparation of aptamer-linked gold nanoparticle purple aggregates for colorimetric sensing of analytes. Nat Protoc 1:246–252. https://doi.org/10.1038/nprot.2006.38
8. Haruta M, Yamada N, Kobayashi T, Iijima S (1989) Gold catalysts prepared by coprecipitation for low-temperature oxidation of hydrogen and of carbon monoxide. J Catal 115:301–309. https://doi.org/10.1016/0021-9517(89)90034-1
9. Hidefumi H, Hitoshi C, Naoki T (1985) Colloidal palladium protected with poly(N-vinyl-2-pyrrolidone) for selective hydrogenation of cyclopentadiene. Makromol Chem Rapid Commun 3:127–141. https://doi.org/10.1016/0167-6989(85)90055-8
10. Angelica B, Cyril G, Carmen C (2011) Pd nanoparticle for C-C coupling reactions. Chem Soc Rev 40:4973–4985. https://doi.org/10.1039/C1CS15195A
11. Yin L, Xiaoyong MH, Davvid MC, Mostafa AES (2000) Suzuki Cross-Coupling Reactions Catalyzed by palladium Nanoparticles in Aqueous Solution. Org Lett 2:2385–2388. https://doi.org/10.1021/ol0061687
12. Axel H, Raphaël S, Denis B, Jaafar G, Jacques L (2005) Heck and Suzuki-Miura coupling catalyzed by nanosized palladium in polyaniline. Appl Organomet Chem 19:1239–1248. https://doi.org/10.1002/aoc.999
13. Chengcai L, Yuhong Z, Yanguang W (2005) Palladium nanoparticles in poly(ethylenglycol): the efficient and recyclable catalyst for Heck reaction. J Mol Catal A 229:7–12. https://doi.org/10.1016/j.molcata.2004.10.039
14. Dipankar S, Ansuman B, Amitabha S (2010) Palladium Nanoparticle Catalyzed Coupling Reaction of Benzyl Halides. J Org Chem 75:4296–4299. https://doi.org/10.1021/jo1003373
15. Pinhua L, Lei W, Hongji L (2005) Application of recoverable nanosized palladium(0) catalyst in Sonogashira reaction. Tetrahedron 61:8633–8640. https://doi.org/10.1016/j.tet.2005.07.013
16. Tobias R, Mehtap O, Peter S (2012) Electrocatalytic Oxygen Evolution Reaction (OER) on Ru, Ir, and Pt Catalysts: A Comparative Study of Nanoparticles and Bulk Materials. ACS Catal 2:1765–1772. https://doi.org/10.1021/cs3003098

17. Sachin K, Shouzhong Z (2009) Electrooxidation of CO on Uniform Arrays of Au Nanoparticles: Effects of Particle Size and Interparticle Spacing. Langmuir 25:574–581. https://doi.org/10.1021/la802747g

18. Hemma M, Farzad B, Rulle R, Ana SV, Peter S, Beatriz RC (2016) Tuning Catalytic Selectivity at the Mesoscale via Interparticle Interactions. ACS Catal 6:1075–1080. https://doi.org/10.1021/acscatal.5b02202

19. Joachim PS, Stefan M, Christoph H, Martin M, Thomas H, Michael K, Hans-Gerd B, Paul Z, Bernd K (2000) Ordered Deposition of Inorganic Clusters from Micellar Block Copolymer Films 16:407–415. https://doi.org/10.1021/la990070n

20. Tianxiang C, Lin Y, Tsz WBL (2021) Designing the electronic and geometric structures of single-atom and nanocluster catalysts. J Mater Chem A 9:18773–18784. https://doi.org/10.1039/D1TA02723A

21. Guoqing W, Hirofumi T, Liu H, Yasutaka M, Kenichi N, Masuhiro A, Kazuhiko M, Takuji O, Kuniharu I (2012) J Mater Chem 22:13691–13697. https://doi.org/10.1039/C2JM31839C

22. Hideki M, Teruoki T, Kazuhiro S, Katsuhiko W, Masahiro K (2006) Network structure consisting of chain-like arrays of gold nanoparticles and silica layer prepared using a nonionic reverse-micell template. J Nanopart Res 8:1083–1087. https://doi.org/10.1007/s11051-006-9070-0

23. Daniel W, Norbert B, Günter S (2002) One-Dimensional Arrangements of Metal Nanoclusters. Nano Lett 2:419–421. https://doi.org/10.1021/nl0157086

24. Haeshin L, Seung HC, Tae GP (2006) Direction Visualization of Hyaluronic Acid Polymer Chain by Self-Assembled One-Dimensional Array of Gold Nanoparticles. Macromolecules 39:23–25. https://doi.org/10.1021/ma051929c

25. Joy YC, Feng Z, Vivian PC, Anne MM, Caroline AR (2006) Self-Assembled One-Dimensional Nanostructure Arrays. Nano Lett 6:2099–2103. https://doi.org/10.1021/nl061563x

26. Hyeong MJ, Ju YK, Minsung H, Seong-Jun J, Bong HK, Seung KC, Kyu HH, Jang HK, Geon GY, Jonghwa S, Sang OK (2018) Ultralarge Area Sub-10 nm Plasmonic Nanogap Array by Block Copolymer Self-Assembly for Reliable High-Sensitivity SERS. ACS Appl Mater Interfaces 10:44660–44667. https://doi.org/10.1021/acsami.8b17325

27. Jeff G, Ji Z, Erik AA, Gabor AS (2002) Ethylene Hydrogenation over Platinum Nanoparticle Array Model Catalysts Fabricated by Electron Beam Lithography: Determination of Active Metal Surface Area. J Phys Chem B 106:11463–11468. https://doi.org/10.1021/jp021641e

28. Bezu T, Stefan F, Kurt VG, Adrian K (2015) Alignment of Gold Nanoparticle-Decorated DNA Origami Nanotubes: Substrate Prepatterning versus Molecular Combing. Langmuir 51:12823–12829. https://doi.org/10.1021/acs.langmuir.5b02569

29. Stephen F, David C, Hakan R, Donald F (2000) Carbon Nnotube Templated Self-Assembly and Thermal Processing of Gold Nanowires. Adv Mater 12:1430–1432. https://doi.org/10.1002/1521-4095(200010)12:19%3c1430::AID-ADMA1430%3e3.0.CO;2-8

30. Taichi M, Mayu H, Hiroaki S, Eiichiro T, Shin-ichiro S (2020) Formation of one-dimensional arrays of nanoparticles using segmented polyurethane nanofibers prepared by electrospinning. Nanotechnology 31:455606. https://doi.org/10.1088/1361-6528/ababca

31. Hiroaki S, Hitoshi A, Takeshi F, Satoshi F, Shin-ichiro S (2014) Atomic force microscopy visualization of hard segment alignment in stretched polyurethane nanofibers prepared by electrospinning. Sci Technol Adv Mater 15:15008–15014. https://doi.org/10.1088/1468-6996/15/1/015008

Publisher's Note Springer Nature remains neutral with regard to jurisdictional claims in published maps and institutional affiliations.